Although membrane tension at the site of ridge contact can only be estimated, calculations (*12*) indicate that the germlings can experience tensions similar to those in patches, provided that signal transduction is limited to a small area such as a small portion of the cell apex. One might suspect that ridges <0.2 or >0.8 μm in height are noninductive for different reasons: too few MS channels may be affected, or contact may be made with an area in which the wall has already polymerized, respectively.

REFERENCES AND NOTES

1. R. W. Emmett and D. C. Parbery, *Annu. Rev. Phytopathol.* **13**, 147 (1975); H. C. Hoch and R. C. Staples, *ibid.* **25**, 231 (1987); in *The Fungal Spore and Disease Initiation in Plants and Animals*, G. T. Cole and H. C. Hoch, Eds. (Plenum, New York, 1991), pp. 25–46.
2. W. K. Wynn, *Phytopathology* **66**, 136 (1976).
3. H. C. Hoch, R. C. Staples, B. Whitehead, J. Comeau, E. D. Wolf, *Science* **235**, 1659 (1987); E. A. Allen *et al.*, *Phytopathology* **81**, 323 (1991).
4. F. Guharay and F. Sachs, *J. Physiol. (London)* **352**, 685 (1984); P. Brehm, Y. Kidokoro, F. Moody-Corbett, *ibid.* **350**, 631 (1984); B. Martinac, M. Buechner, A. H. Delcour, J. Adler, C. Kung, *Proc. Natl. Acad. Sci. U.S.A.* **84**, 2297 (1987); W. J. Sigurdson, C. E. Morris, B. L. Brezden, D. R. Gardner, *J. Exp. Biol.* **127**, 191 (1987); J. B. Lansman, T. J. Hallam, T. J. Rink, *Nature* **325**, 811 (1987); H. Sackin, *Proc. Natl. Acad. Sci. U.S.A.* **86**, 1731 (1989); X.-C. Yang and F. Sachs, *Science* **243**, 1068 (1989); B. Martinac, J. Adler, C. Kung, *Nature* **348**, 261 (1990).
5. M. C. Gustin, X.-L. Zhou, B. Martinac, C. Kung, *Science* **242**, 762 (1988).
6. Urediospores (0.5 g) were germinated in water at 16° to 19°C until the germ tubes were 40 to 70 μm long (~2 hours) and before all of the cytoplasm had migrated out of the spore. To produce protoplasts, germlings were digested for 25 to 40 min with Novozyme (Novo BioLabs, Bagsvaerd, Denmark), 5 mg/ml, in 0.5-M sorbitol buffered with 17 mM MES, pH 6.0 [D. Huang, R. C. Staples, W. R. Bushnell, D. L. Maclean, *Phytopathology* **80**, 81 (1990)]. All protoplasts were formed from the germling apices. After filtration through a 20-μm mesh Nytex cloth (Tetko, Inc., Elmsford, NY), the protoplasts were pelleted at 2000*g* for 4 min and resuspended in sorbitol without enzyme. The protoplasts were washed twice through centrifugation in the recording bath solution (7). Protoplasts selected for patch-clamping appeared uniformly dark, smooth, and empty when viewed with phase contrast optics.
7. The protoplast membrane of *U. appendiculatus* (*6*) formed gigaohm seals more easily than that of *Saccharomyces cerevisiae*. After seal formation, we were often confronted with cell-attached patches, in which the MS channels could be activated with large suctions, albeit the activities were not as clear as in other modes. For *U. appendiculatus* protoplasts, a 10- to 30-mmHg suction sustained over several minutes, instead of pulses of very large suctions, was most effective in converting the cell-attached mode to whole-cell mode. Whole-cell current through the MS channels was verified with a small positive pressure. Once established, the whole-cell preparation usually lasted for hours. Pressure application, pressure measurement, and recording, digitizing, and analyzing of data have been reported (*5*). Unless stated otherwise, the bath solution was 220-mM KCl, 50-mM $MgCl_2$, 5-mM Hepes, pH 7.2, and the pipette solution was 290-mM KCl, 10^{-2}- mM $CaCl_2$, 5-mM Hepes, pH 7.2 (pH adjusted with KOH).
8. C. E. Morris and R. Horn, *Science* **251**, 1246 (1991).
9. S. G. Spangler, *Ala. J. Med. Sci.* **9**, 218 (1972).
10. M. A. Stumpf, unpublished results.
11. Y. Kwon, H. C. Hoch, J. R. Aist, *Can. J. Bot.*, in press.
12. The membrane tension (T) is related to applied pressure (P) according to Laplace's law: $T = Pd/4$, where d is the cell diameter. Low but significant channel opening was observed at a pressure of 10 mmHg in protoplasts with an estimated diameter of 4 to 7 μm. The resulting values for T are 1.3×10^{-3} to 2.3×10^{-3} N/m. In germ tubes, the tension experienced on contact with a ridge can be calculated as follows: $T = K_A \Delta A/A$, where K_A is the area elasticity and ΔA is the change in the area (A) experiencing the tension (*13*). If tension from the observed membrane deformation [Y. H. Kwon, thesis, Cornell University (1991)] is experienced over the whole germ tube membrane, then $\Delta A/A$ is negligible. With a K_A of 100×10^{-3} N/m, representative of most biological lipids (*13*), the tension in germ tubes is far less than that which opened channels in patched protoplasts. However, the region of deformation on contact is limited; therefore, a tension of approximately 2.1×10^{-3} N/m is produced. The K_A would be larger for membranes with underlying cytoskeleton, thus the value calculated for T in the germlings could be underestimated.
13. F. Sachs, in *Ionic Channels in Cells and Model Systems*, R. Latorre, Ed. (Plenum, New York, 1986), pp. 181–193.
14. Channel activity was quantified as $Np_0 = \Sigma_{n=1}^{N} np_n$, where p_0 is the open probability of the single channel, p_n is the probability that n channels are open simultaneously, and the N is the apparent number of channels. The value of p_n was derived as in Fig. 2B. The observed occupancies of conductance levels zero through six were 0.156, 0.287, 0.303, 0.199, 0.037, 0.009, and 0.008. This distribution can be fitted to a Poisson distribution of $p_k = (\lambda^K e^{-\lambda})/K!$ (K = 0,1, . . .,6), where $Np_0 = \lambda$. The first seven terms of this Poisson distribution are 0.177, 0.306, 0.265, 0.153, 0.066, 0.029, and 0.008. The observed distribution does not differ significantly from that calculated in a χ^2 test.

15. We thank B. Martinac, P. Minorsky, R. C. Staples, W. Sigurdson, and F. Sachs for valuable discussions. Programs used to analyze single-channel records were developed by Y. Saimi. Supported by the Lucille P. Markey Trust (C.K.) and the NSF (H.C.H.).

29 March 1991; accepted 10 June 1991

Depletion of CD4$^+$ T Cells in Major Histocompatibility Complex Class II–Deficient Mice

MICHAEL J. GRUSBY, RANDALL S. JOHNSON, VIRGINIA E. PAPAIOANNOU, LAURIE H. GLIMCHER*

The maturation of T cells in the thymus is dependent on the expression of major histocompatibility complex (MHC) molecules. By disruption of the MHC class II A^b_β gene in embryonic stem cells, mice were generated that lack cell surface expression of class II molecules. These MHC class II–deficient mice were depleted of mature CD4$^+$ T cells and were deficient in cell-mediated immune responses. These results provide genetic evidence that class II molecules are required for the maturation and function of mature CD4$^+$ T cells.

THE NORMAL DEVELOPMENT OF MATURE CD4$^+$ T lymphocytes requires their interaction with MHC-encoded class II molecules in the thymus (*1–6*). These polymorphic molecules are present on thymic cortical epithelial cells, and their engagement with the αβ T cell receptor on immature thymocytes is thought to result in the positive selection of CD4$^+$ T cells and their ultimate export to the periphery (*4–7*). Gene targeting (*8*) is a method by which specific genes can be altered in embryonic stem (ES) cells regardless of their expression (*9*) and subsequently passed through the germ line (*10–17*). We have used this technique to generate mice that are devoid of cell surface expression of MHC class II molecules by introducing a loss of function mutation into the A^b_β gene (*18*) in ES-D3 cells. ES-D3 cells are derived from mice of the H-2^b haplotype (*19*) and thus harbor a deletion in their E^b_α gene that prevents the expression of I-E molecules on the surface of class II expressing cells (*20*). Disruption of the A^b_β gene in ES-D3 cells would similarly prevent the cell surface expression of I-A molecules on class II expressing cells. Therefore, mice of this genotype should be deficient in the cell surface expression of both I-E and I-A class II MHC molecules.

The targeting vector (Fig. 1A) incorporates the neomycin resistance (*neo*^{r}) gene into the second exon of the A^b_β gene, contains 5.4 kb of homologous flanking sequence, and contains the herpes simplex virus (HSV-1) thymidine kinase (*tk*) gene, allowing positive-negative selection of transfectants (*21*). Of the 2×10^7 ES-D3 cells transfected with this construct, 720 colonies were G418^r (calculated from control plates), whereas 143 were resistant to both G418 and gancyclovir. Of these 143 colonies, 86 were screened by Southern (DNA) blot analysis and four clones contained a disrupt-

M. J. Grusby and L. H. Glimcher, Department of Cancer Biology, Harvard School of Public Health, and Department of Medicine, Harvard Medical School, Boston, MA 02115.
R. S. Johnson, Dana-Farber Cancer Institute and Department of Biological Chemistry and Molecular Pharmacology, Harvard Medical School, Boston, MA 02115.
V. E. Papaioannou, Department of Pathology, Tufts University School of Medicine and Veterinary Medicine, Boston, MA 02111.

*To whom correspondence should be addressed.

ed A^b_β gene. One clone containing a disrupted A^b_β gene was injected into C57BL/6J blastocysts. Fifteen mice were born out of 39 embryos transferred to recipients that became pregnant. Of these 15 animals, seven males and one female were chimeric. Two males out of the three test bred transmitted the ES cell genotype, one to <1% and the other to 28% of their offspring. Half of the progeny carried the disrupted A^b_β allele as determined by Southern blot analysis of DNA obtained from tail biopsies. Heterozygous offspring were then mated to yield (129/Sv × C57BL/6J)F_2 animals, some of which were homozygous for the disrupted A^b_β allele (Fig. 1B). The F_2 animals were raised under germ-free conditions and appeared healthy. The animals used for the experiments described were between 5 and 6 weeks of age.

To assess the effect of this mutation on MHC class II expression, we examined frozen sections of thymus from wild-type (+/+) or mutant (−/−) animals by immunohistochemistry using the A^b_β-specific monoclonal antibody (MAb) 25-9-17. Wild-type thymic sections had a characteristic reticular pattern of staining in the cortex with a more uniform staining in the medulla (Fig. 2A). In contrast, thymic sections from animals homozygous for the disrupted A^b_β allele had no specific staining either in the cortical or medullary regions (Fig. 2B), as similar background staining was seen with the 25-9-17 MAb on thymic sections from a mouse of the H-2^k haplotype (*22*). Furthermore, flow cytometric analysis of lymphocytes from spleen and lymph nodes with MAbs to A^b_β (25-9-17 and 34-5-3) and A^b_α (3JP and 1E9) showed an absence of I-A antigens on lymphoid cells in the periphery of animals homozygous for the disrupted A^b_β allele (Fig. 3, C and D). Although these H-2^b animals do not express class II I-E antigens due to a deletion in their E^b_α gene (*20*), it was formally possible that expression of the functional E^b_β and A^b_α genes could result in the mixed isotypic molecule $E^b_\beta A^b_\alpha$ on the cell surface. Flow cytometric analysis of lymphoid cells with either A^b_α-specific MAbs (Fig. 3, C and D) or the E^b_β-specific MAb Y17 (*22*) did not detect this mixed isotypic molecule. Although we cannot rule out the possibility that these antibodies, generated against the $A^b_\beta A^b_\alpha$ or $E^b_\beta E^b_\alpha$ molecule, do not recognize the $E^b_\beta A^b_\alpha$ molecule, this mixed isotypic pair has not been observed at the cell surface of bulk transfected L cells (*23*). Flow cytometric analysis with MAbs to the class I K^b molecule and immunoglobulin M indicated normal levels of these surface markers on cells from the spleen, thymus, and lymph nodes of class II–deficient animals (*22*).

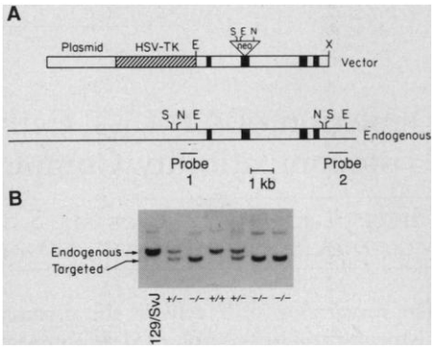

Fig. 1. Gene targeting of the A^b_β gene and germ line transmission of the disrupted allele. (**A**) A schematic of the gene targeting construct used for disruption of the A^b_β gene is shown above the endogenous A^b_β gene. Black boxes represent exons, and restriction enzyme sites are as indicated. A 5.4-kb Eco RI–Xho I fragment of the A^b_β gene encompassing the first four exons was subcloned into a pBluescript SK (+) vector into which a 3.4-kb Bam HI fragment of HSV-1 containing the *tk* gene was previously blunt-cloned into the Nae I site (*9*). The unique Bst EII restriction enzyme site in the second exon of the A^b_β gene was changed to a Sal I site with linkers and the 1.1-kb Xho I–Sal I fragment of pMC1neo-poly A (Stratagene) containing the neo^r gene was inserted into this site. ES-D3 cells (2×10^7) in 0.8 ml of PBS were transfected with Not I linearized DNA (20 μg) with a Bio-Rad Gene Pulser (25 μF/0.35 kV) and plated in ten 150-mm petri dishes in media (Dulbecco's minimum essential medium with 20% fetal calf serum, 2 mM glutamine, 0.1 mM nonessential amino acids, and 0.1 mM 2-mercaptoethanol) supplemented with leukemia inhibitory factor–containing supernatants. Media with Geneticin (150 μg/ml; Gibco) and gancyclovir (2 μM; Syntex, Palo Alto, California) was added 24 hours after transfection and drug selection continued for 9 days. Genomic DNA was prepared from individual colonies and analyzed by Southern blot with the indicated probes. Probe 1 is a 690-bp Bgl II–Eco RI fragment that hybridizes to a 6.3-kb Nco I fragment of the endogenous A^b_β gene and to a 3.8-kb fragment of the disrupted allele resulting from homologous recombination with the depicted targeting construct (*22*). Probe 2 is a 705-bp Xho I–Eco RI fragment that hybridizes to a 6.4-kb Eco RI fragment of the endogenous A^b_β gene and 5.2-kb fragment of the disrupted allele. (**B**) Southern blot analysis of tail DNA from several animals in a litter derived from a heterozygous mating pair results in the identification of animals that are homozygous wild type (+/+), heterozygous (+/−), or homozygous for the disrupted A^b_β allele (−/−). DNA was digested with Eco RI and hybridized with probe 2. Restriction sites are Eco RI (E), Nco I (N), Stu I (S), and Xho I (X).

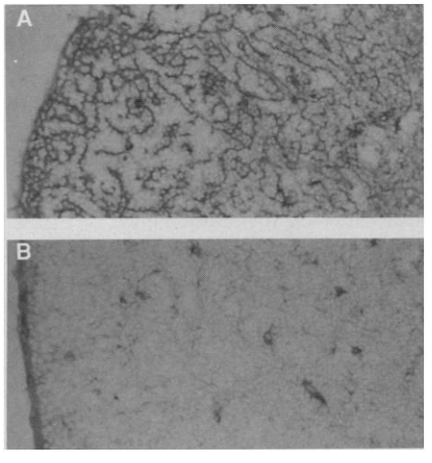

Fig. 2. Immunohistochemistry of thymic sections from class II–deficient mice. Frozen sections (6 μm) of thymus from (**A**) wild-type (+/+) and (**B**) mutant (−/−) mice were hydrated in 0.05 M tris-HCl, pH 7.5, for 5 min and then blocked with 3% horse serum for 15 min. Sections were incubated with purified A^b_β specific MAb 25-9-17 (diluted in horse serum) for 60 min, then with biotinylated horse antibody to mouse IgG and avidin-horseradish peroxidase as described by the manufacturer (Vectastain Elite ABC kit, Vector Laboratories). Stained sections were developed with 3,3′-diaminobenzidine as chromogen for 4 min. Thymic sections from wild-type (+/+) mice showed a reticular pattern of staining in the cortex with the A^b_β-specific MAb characteristic of cortical epithelial cells. This staining is absent on thymic sections from class II–deficient (−/−) animals. Thymic sections from class II–deficient animals had even lower background staining with immunoperoxidase than do thymic sections from CBA/J animals of the H-2^k haplotype (*22*).

Neonatal treatment of mice with antibodies specific for class II molecules arrests the development of $CD4^+$ T cells in the thymus (*1*). We, therefore, examined the composition of thymocyte subsets in class II–deficient animals. Two-color flow cytometric analysis of thymocyte subsets in mutant mice revealed a reduction in the number of single positive $CD4^+$ cells in the thymus (0.6% versus 9.9% in control animals) (Fig. 4A). In contrast, the number of double positive $CD4^+CD8^+$ cells in mutant mice is equivalent to that seen in control animals. These results imply that the expression of CD4 during T cell maturation in the thymus does not require the presence of I-A and I-E class II molecules, but that progression from the double-positive $CD4^+CD8^+$ stage to the single-positive $CD4^+$ stage does.

Examination of single-positive $CD8^+$ T cells in the thymus and periphery of class II–deficient animals shows elevated numbers of these cells relative to control littermates (Fig. 4, A and B). It is possible that the $CD8^+$ T cell population expands because of the deficit of $CD4^+$ cells. However, β_2-microglobulin (MHC class I)–deficient mice that lack $CD8^+$ T cells do not have elevated numbers of $CD4^+$ cells (*24, 25*). The number of single positive $CD4^+$ cells in the periphery of class II–deficient mice is reduced in comparison to control littermates (Fig. 4B). In contrast to the thymus, however, there are detectable numbers of $CD4^+$

cells in the periphery (3.2%). Although the nature of this population is unclear, it is possible that these cells represent either class I–restricted $CD4^+$ T cells, $CD4^+$ γδ T cell receptor–bearing T cells, or $CD4^+$ natural killer–like cells. Another possibility is that this small population of $CD4^+$ cells is restricted to a novel MHC class II molecule, H-2O, whose distribution in the thymus and periphery differs from classical MHC class II antigens (*26*).

In order to determine the functional consequences of MHC class II deficiency, we examined animals for their ability to mount an antigen-specific antibody response. Sera from control and mutant animals immunized with trinitrophenol (TNP)-conjugated ovalbumin were assayed by enzyme-linked immunosorbent assay (ELISA) to determine the isotype profile of TNP-specific antibody produced (Table 1). Although control animals produced immunoglobulins (Ig) IgG_1, $IgG2_a$, $IgG2_b$, and IgG_3 specific for TNP 12 days after immunization, class II–deficient animals did not make immunoglobulins of these isotypes. In contrast, both control and mutant animals produced IgM TNP-specific antibodies, with consistently higher titers (even in preimmune sera) in mutant animals than in control littermates.

Table 1. ELISA analysis of TNP-specific antibody in class II–deficient animals. Animals were immunized with TNP-OVA (300 μg in complete Freund's adjuvant) and bled 12 days after immunization. Dilutions (Diln) of sera were analyzed by ELISA with alkaline phosphatase-conjugated isotype-specific reagents (Southern Biotechnology Associates). Absorbance at 405 nm is given. The data shown are from one control and one mutant animal and are representative of three experiments.

Diln	IgM		IgG_1		IgG_{2a}		IgG_{2b}		IgG_3	
	Pre	Post	Pre	Post	Pre	Post	Pre	Post	Pre	Post
					Control serum					
1:100	0.094	0.116	0.010	0.642	0.064	0.784	0.040	0.775	0.006	0.132
1:1000	0.012	0.014	0.033	0.168	0.028	0.150	0.007	0.070	0.002	<0.001
1:10,000	0.018	<0.001	0.050	0.012	0.023	0.007	0.002	0.005	0.001	<0.001
					Mutant serum					
1:100	0.338	0.480	0.028	0.034	0.033	0.040	0.003	<0.001	0.014	0.027
1:1000	0.042	0.020	0.016	0.018	0.010	0.008	<0.001	<0.001	0.012	<0.001
1:10,000	<0.001	<0.001	0.043	0.002	0.001	<0.001	<0.001	<0.001	0.014	<0.001

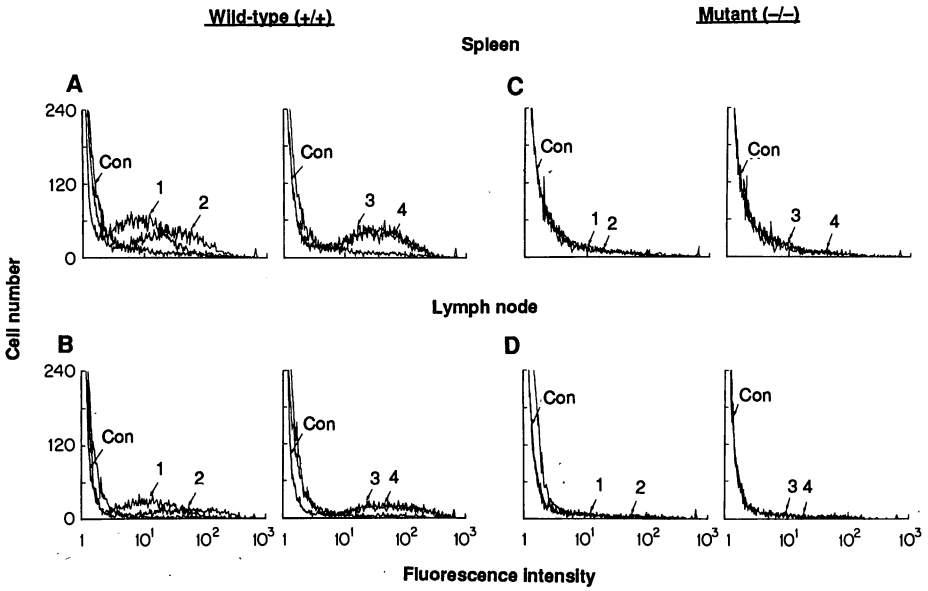

Fig. 3. Flow cytometric analysis of MHC class II expression in the periphery of class II–deficient animals. Single-cell suspensions were prepared from spleens and lymph nodes of (**A** and **B**) wild-type (+/+) or (**C** and **D**) mutant (−/−) animals and 1.5 × 10^6 cells were stained with hybridoma supernatant containing class II–specific antibodies. MAbs were 25-9-17 and 34-5-3 (A^b_β), and 3JP and 1E9 (A^b_α). Cells were washed once in Hanks basic salt solution, 3% fetal calf serum, and 0.1% NaN_3 and then incubated with fluorescein-conjugated $F(ab')_2$ fragment of goat antibody to mouse IgG (γ-chain–specific) (Cappel). Cells were then washed, fixed in 2% paraformaldehyde, and analyzed by flow cytometry on a Coulter 752 (Coulter Electronics). Control shows background staining obtained with the secondary reagent alone. Flow cytometric analysis was performed three separate times with one wild-type and one mutant animal, each time yielding essentially identical results. 1, 25-9-17 MAb; 2, 34-5-3 MAb; 3, 1E9 MAb; and 4, 3JP MAb.

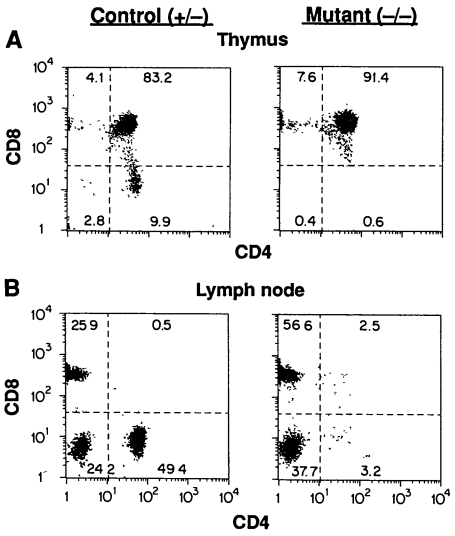

Fig. 4. Flow cytometric analysis of lymphocyte subsets in class II–deficient animals. Single cell suspensions were prepared from thymus (**A**) and lymph nodes (**B**) of control (+/−) or mutant (−/−) animals and analyzed as in Fig. 3 except that a FACScan (Becton Dickenson) flow cytometer was used. Fluorescein-conjugated anti-CD4 and phycoerythrin-conjugated anti-CD8 were from Pharmingen. Flow cytometric analysis was performed four separate times with one control (+/+ or +/−) and one mutant (−/−) animal each time yielding essentially identical results. Number of events counted: lymph node, 25,000; thymus, 50,000.

That the T cell compartment in mutant animals is not completely anergic to stimulation could be demonstrated by the equivalent proliferative responses exhibited by these cells to stimulation with CD3 antibody or concanavalin A as compared to lymphocytes from control animals (*22*). These results are consistent with the notion that class switching from IgM to IgG isotypes requires cognate interactions between $CD4^+$ T cells and antigen-specific B cells. Because these mutant animals are both deficient for class II expression and depleted of $CD4^+$ cells, additional studies will be required to determine the contribution of each of these defects to the failure to undergo isotype switching. Finally, preliminary studies suggest that the ability of class II–deficient animals to reject allografts is significantly impaired, as minor histocompatibility complex disparate grafts survive approximately three times longer on mutant animals relative to control animals (*27*).

In summary, we have used gene targeting in ES cells to generate mutant mice that are deficient in cell surface expression of MHC class II molecules. Our data provide genetic evidence for the essential role of these molecules in the development and function of $CD4^+$ T cells. These class II–deficient animals do have small numbers of $CD4^+$ T cells in their spleen and lymph nodes, and the phenotype of these cells will require further

examination. Finally, these animals will serve as useful recipients for the reintroduction of class II molecules targeted to specific locations in order to better understand the role of these proteins in various autoimmune phenomena.

REFERENCES AND NOTES

1. A. M. Kruisbeek *et al.*, *J. Exp. Med.* **161**, 1029 (1985).
2. H. S. Teh *et al.*, *Nature* **335**, 229 (1988).
3. B. Scott, H. Bluthmann, H. S. Teh, H. von Boehmer, *ibid.* **338**, 591 (1989).
4. C. Benoist and D. Mathis, *Cell* **58**, 1027 (1989).
5. J. Bill and E. Palmer, *Nature* **341**, 649 (1989).
6. L. J. Berg *et al.*, *Cell* **58**, 1035 (1989).
7. W. van Ewijk *et al.*, *ibid.* **53**, 357 (1988).
8. K. R. Thomas and M. R. Capecchi, *ibid.* **51**, 503 (1987).
9. R. S. Johnson *et al.*, *Science* **245**, 1234 (1989).
10. S. Thompson, A. R. Clarke, A. M. Pow, M. L. Hooper, D. W. Melton, *Cell* **56**, 313 (1989).
11. M. Zijlstra, E. Li, F. Sajjadi, S. Subramani, R. Jaenisch, *Nature* **342**, 435 (1989).
12. T. M. DeChiara, A. Efstratiadis, E. J. Robertson, *ibid.* **345**, 78 (1990).
13. A. P. McMahon and A. Bradley, *Cell* **62**, 1073 (1990).
14. P. Soriano, C. Montgomery, R. Geske, A. Bradley, *ibid.* **64**, 693 (1991).
15. O. Chisaka and M. R. Capecchi, *Nature* **350**, 473 (1991).
16. W.-P. Fung-Leung *et al.*, *Cell* **65**, 443 (1991).
17. D. Kitamura, J. Roes, R. Kuhn, K. Rajewsky, *Nature* **350**, 423 (1991).
18. D. Larhammar *et al.*, *Cell* **34**, 179 (1983).
19. T. C. Doetschman, H. Eistetter, M. Katz, W. Schmidt, R. Kemler, *J. Embryol. Exp. Morph.* **87**, 27 (1985).
20. D. J. Mathis, C. Benoist, V. E. Williams, M. Kanter, H. O. McDevitt, *Proc. Natl. Acad. Sci. U.S.A.* **80**, 273 (1983).
21. S. L. Mansour, K. R. Thomas, M. R. Capecchi, *Nature* **336**, 348 (1988).
22. M. Grusby, unpublished observation.
23. R. Germain, personal communication.
24. M. Zijlstra *et al.*, *Nature* **344**, 742 (1990).
25. B. H. Koller, P. Marrack, J. W. Kappler, O. Smithies, *Science* **248**, 1227 (1990).
26. L. Karlsson, C. D. Surh, J. Sprent, P. A. Peterson, *Nature* **351**, 485 (1991).
27. H. Auchincloss, unpublished observation.

28. We thank L. Jackson-Grusby for advice and help in preparation of the manuscript, H. Auchincloss for performing the allografts, J. Markowitz for assisting with FACS and ELISA, R. Kemler for ES-D3 cells, G. Wong for LIF supernatants, J. Darling, M. McLane, J. Spencer, B. van Lingen, A. Abbas, and H. Burstein for technical assistance, C. Kara for helpful discussions, and B. Spiegelman for advice and encouragement. Supported by NIH grants AI21569 (L.H.G.) and HD27295 (V.E.P.), the Arthritis Foundation (M.J.G.), and the Leukemia Society of America (M.J.G. and L.H.G.).

18 July 1991; accepted 23 August 1991

Excitatory Synaptic Responses Mediated by $GABA_A$ Receptors in the Hippocampus

HILLARY B. MICHELSON AND ROBERT K. S. WONG

Gamma-aminobutyric acid (GABA) is a major inhibitory neurotransmitter in the cortex. Activation of postsynaptic $GABA_A$ receptors hyperpolarizes cells and inhibits neuronal activity. Synaptic responses mediated by $GABA_A$ receptors also strongly excited hippocampal neurons. This excitatory response was recorded in morphologically identified interneurons in the presence of 4-aminopyridine or after elevation of extracellular potassium concentrations. The synaptic excitation sustained by $GABA_A$ receptors synchronized the activity of inhibitory interneurons. This synchronized discharge of interneurons in turn elicited large-amplitude inhibitory postsynaptic potentials in pyramidal and granule cells. Excitatory synaptic responses mediated by $GABA_A$ receptors may thus provide a mechanism for the recruitment of GABAergic interneurons through their recurrent connections.

STUDIES OF THE CELLULAR AND CIRcuit properties of the hippocampus have focused primarily on the output excitatory neurons, the pyramidal cells. Inhibitory GABAergic interneurons are the other major cell type in the hippocampus (*1*). The features of these inhibitory cells are not as well characterized as those of the pyramidal cells, presumably because it is difficult to obtain intracellular recordings from these sparsely distributed elements (*2*). During normal activity, interneurons are activated by afferent fibers (feedforward inhibition) (*3*) and by recurrent axons of pyramidal cells (feedback inhibition) (*4*). Excitation through these pathways is mediated by glutamatergic synapses. However, recent studies in the cortex (*5*) suggest that another mechanism, independent of glutamatergic transmission, may be involved in the synchronization of GABAergic interneurons.

We investigated the glutamate-independent recruitment of interneurons by recording intracellularly from pyramidal cells and interneurons in the hippocampal slice (*6*). In the presence of the convulsant compound 4-aminopyridine (4-AP) (50 to 100 μM) and excitatory amino acid (EEA) receptor blockers (*7*) [3-(2-carboxypiperazin-4-yl)propyl-1-phosphonic acid (CPP), 10 to 30 μM, and 6-cyano-7-nitroquinoxaline-2,3-dione (CNQX), 10 μM], rhythmic, synchronized inhibitory postsynaptic potentials (IPSPs) (*7* to 15 mV peak amplitude; up to 900 ms in duration) occurred in pyramidal and granule cells. These events occurred at frequencies ranging from 0.1 to 0.3 Hz (*8*).

To explore the origin of the synchronized IPSPs, we obtained intracellular recordings from GABAergic interneurons. The hilar region of the dentate gyrus is particularly suitable for such a study. A dense population of GABAergic interneurons is located in an identifiable site that is distinct from the granule-cell layer and devoid of granule-cell dendrites (*9*). In the presence of 4-AP and EAA receptor blockers, intracellular recordings obtained from electrodes placed in stratum pyramidale or within the granule cell layer consistently revealed spontaneous, synchronized IPSPs. In contrast, in a large proportion of intracellular recordings (80%) from neurons within a specific region of the hilus (see Fig. 1), we saw spontaneous, rhythmic bursts of action potentials. Simultaneous recordings indicated that bursts in these hilar cells occurred simultaneously with synchronized IPSPs in principal (pyramidal and granule) cells (Fig. 1A). Recordings from pairs of hilar cells demonstrated that burst firing occurred simultaneously in these neurons (Fig. 1A). Thus, we named the depolarizing events in hilar cells synchronized bursts.

Spontaneous synchronized bursts in hilar interneurons and corresponding synchronized IPSPs were also recorded in the presence of EAA receptor blockers when the extracellular potassium concentration ($[K^+]_o$) was raised from 5 to 12 mM (*10*) (Fig. 1B). Synchronized events recorded in the high $[K^+]_o$ condition occurred sporadically. However, they could be triggered consistently by electrical stimulation applied at frequencies lower than 0.2 Hz (see below).

We visualized hilar neurons that had the above described electrophysiological properties. Recording electrodes containing the fluorescent dye Lucifer yellow (LY) were used, and cells of interest were filled with the dye (*6*). Eleven bursting hilar cells were filled with LY (Fig. 1C). All of the filled cells were nonpyramidal and shared some common morphological features. The somata of these cells were typically ovoid in shape, with dendrites preferentially extending in a plane parallel to the granule cell layer. The shape of these cells resembled that of horizontal cells. Horizontal-type cells in the hilar region are positively stained by antibodies to glutamic acid decarboxylase, the synthetic enzyme for GABA, suggesting that they are GABAergic neurons (*11*).

Department of Pharmacology, State University of New York, Health Science Center, Brooklyn, NY 11203.